Use of chromatographic and electrophoretic tools for assaying elastase, collagenase, hyaluronidase, and tyrosinase activity

Syntia Fayad, Philippe Morin, Reine Nehmé

Use of chromatographic and electrophoretic tools for assaying elastase, collagenase, hyaluronidase, and tyrosinase activity

*Syntia Fayad, Philippe Morin, Reine Nehmé**

Institut de Chimie Organique et Analytique (ICOA), Université d'Orléans – CNRS, UMR 7311, Orléans, France

* Corresponding author: Dr. Reine Nehmé, Institut de Chimie Organique et Analytique (ICOA), Université d'Orléans, BP 6759, rue de Chartres, 45067 Orléans cedex 2, France.
e-mail: reine.nehme@univ-orleans.fr ; Tel: +33-2-38-49-27-75 ; Fax: +33-2-38-41-72-81

List of abbreviations: **BGE:** background electrolyte; **BTH:** bovine testicular hyaluronidase; **CS:** chondroitin sulfate; **ECM:** extracellular matrix; **EMMA**, electrophoretically mediated microanalysis; **FAC:** frontal analysis chromatography; **HA**, hyaluronic acid; **HNE**, human neutrophil elastase; **Hyal,** hyaluronidase**; IB:** incubation buffer; **LIF**, laser induced fluorescence; **MMP,** matrix metalloproteinases; **MST:** microscale thermophoresis; **PMMA,** pressure-mediated microanalysis; **SFE:** skin fibroblast elastase; **TDLFP**, transverse diffusion of laminar flow profiles; **Tyr,** tyrosinase.

Keywords: Capillary electrophoresis, enzymatic assays, high performance liquid chromatography, microscale thermophoresis, kinetic constants

ABSTRACT

Elastase, collagenase, hyaluronidase and tyrosinase, are very interesting enzymes due to their direct implication in skin aging and as therapeutic hits. Different techniques can be used to study these enzymes and to evaluate the influence of effectors on their kinetics. Nowadays, analytical techniques have become frequently used tools for miniaturizing enzyme assays. The main intention of this article is to review chromatographic and electrophoretic tools that study the four enzymes above mentioned. More specifically, the use of high-performance liquid chromatography and capillary electrophoresis and their derivative techniques for monitoring these enzymes will be investigated. The advantages and limitations of these assays will also be discussed. The original use of microscale thermophoresis and thin layer chromatography in this domain will also be covered.

1. Introduction

The skin is composed of three layers; the epidermis, dermis and the subcutaneous layer [1]. The extracellular matrix (ECM) is the outermost part of the skin and contains essential components for wound healing [2]. The molecules associated with the ECM of each tissue, including collagens, proteoglycans, laminins and fibronectin, and the manner in which they are assembled determine the structure and the organization of the ECM [3]. The degradation of ECM is thus linked to skin aging. Different intrinsic and extrinsic factors can affect the skin and cause its damage [4, 5]. Intrinsic structural changes occur as a natural consequence of aging and are genetically determined while extrinsic factors are, to varying degrees, controllable. The extrinsic agents include exposure to UV sunlight, pollution or nicotine, repetitive muscle movements like squinting or frowning, and miscellaneous lifestyle components such as diet, sleeping position, and overall health [6-8]. Solar radiation can damage human skin such as an acute overexposure that causes clinical sunburn. Chronic exposure can lead to skin changes such as plaque-like thickening, loss of skin tone, deep furrowing and fine wrinkle formation. Collectively, these changes may be termed ‘photoaged skin’ or ‘solar scar’. The solar UV radiation has particularly a negative effect on the health of the skin, since they involve the generation of reactive oxygen (ROS) species and cellular oxidative damage [9]. Figure 1 shows the induction of skin aging caused by environmental factors and more specifically by solar UV. The generated ROS induce angiogenesis, which is the process of generating new blood vessels [10, 11]. However, the blood vessels are also decreased in chronically UV-damaged human skin. This damage is known to result in marked degenerative changes of the upper dermal connective tissue with degradation of elastic fibers, collagen fibers and hyaluronic acid (Figure 2). This is probably due to increased expression of elastase, matrix metalloproteinase (MMP), and hyaluronidase (hyal) produced in keratinocytes, fibroblasts and various inflammatory cells (Figure 1). On the other hand, UV sunlight and ROS activates melanogenesis, which is the process of melanin production and distribution [12-14]. Tyrosinase (tyr), the key protein involved in skin pigmentation due to the presence of melanin pigment, is activated and a hyperpigmentation is produced [12]. Therefore, understanding the evolution of enzymes in the human body is important to understand and to find new therapeutics for a broad range of biological phenomena [15, 16].

Elastase, known for its capacity to cleave proteins, prefers the amino acids valine and alanine (Figure 2.a). Available evidence suggests that there are at least two main types of elastases implicated in the skin degradation, human neutrophil elastase (HNE) and skin fibroblast elastase (SFE). HNE is derived from neutrophil cells and SFE from fibroblasts and these two differ in their substrate specificity [17]. HNE is a 29 kD serine endoprotease of the proteinase S1 family. It exists as a single 238 amino acid-peptide chain with four disulfide bonds and contains two or three N-linked glycans of variable composition that account for its three major isoforms with an isoelectric point of 8.77 - 9.55. Natural substrates include elastin, cartilage proteoglycans, collagen types I, II, III and IV, and fibronectin [18]. SFE has been characterized as a membrane-

bound metalloproteinase with little information about its structure, amino acid sequence, and encoding gene. It acts on oxytalan fibers and elaunin fibers but has limited effects on mature elastic fibers. Several studies suggests that SFE is identical to neprilysin, (neutral endopeptidase 24.11 or NEP) due to similarities in their molecular weights and activity profiles [19, 20]. HNE and SFE are also implicated in the metabolism of elastic fibers in various types of tissues during inflammation or diseases [21, 22].

The matrix metalloproteinases (MMPs) are a family of zinc and calcium dependent enzymes which are important in the resorption of ECM in normal physiological processes and pathological states [7]. These enzymes are responsible for the degradation of ECM molecules and are also implicated in the tissue remodeling, which accompanies inflammation, bone resorption, atherosclerosis, and the invasion of tumors [23]. Most of collagnases belongs to the MMP family. Collagenases are responsible for collagen degradation by breaking the peptide bonds (Figure 2.b). Collagen is the major insoluble fibrous protein in the ECM and the connective tissue and its primary function is to maintain skin firmness. Sixteen types of collagen exist and around 80 – 90 % of the collagen in human body only consists of types I, II, and III. Different types of collagenases exist like gelatinase B, which cleaves gelatine type I and collagen types IV and V, gelatinase A which cleaves gelatine type I and collagen types IV, V, VII and X and neutrophil collagenase which cleaves interstitial collagens with a preference for collagen type I [24].

Skin aging is also associated with loss of skin moisture where the most important key molecule involved is hyaluronic acid (HA). This high molecular weight mucopolysaccharide (1.5-1.8 x 10^6 Da) was discovered in 1934 by Karl Meyer in the vitreous of bovine eyes [25]. This non-sulphated glycosaminoglycan is composed of repeating polymeric disaccharides of D-glucuronic acid and N-acetyl-D-glucosamine linked by a glucuronidic β (1→3) bond (Figure 2.c) [26]. Its function is, amongst other things, to bind water and to lubricate movable parts of the body, such as joints and muscles. Its consistency and tissue-friendliness allow it therefore to be beneficial in skin-care products as an excellent moisturizer. This acid is naturally synthesized by a class of integral membrane proteins called hyaluronan synthases, and degraded by a family of enzymes called hyaluronidases or Hyal [27], which display both hydrolytic and transglycosylation activities. In the presence of NaCl, at pH 4-5 and at 37°C, Hyal mainly catalyzes a hydrolysis reaction with a preference for HA over chondroitin sulfate (CS). In the absence of NaCl, at higher pH of 7 and at 37°C or higher, Hyal mainly catalyzes a transglycosylation reaction and prefers CS over HA [28, 29]. In the human genome, six Hyal sequences occur with similar catalytic mechanisms. The most recent overview dealing with these enzymes was prepared in 2008 by Stern el al [30].

Tyrosinase is present in melanosome granules present in melanocytes. This multifunctional, glycosylated, and copper-containing oxidase catalyzes the first of the two steps in mammalian melanogenesis. This is the entire process leading to the formation of dark macromolecular pigments, like melanin in the skin. Melanogenesis is initiated with the first step of tyrosine oxidation to dopaquinone catalyzed by Tyr (Figure 2.d). In mammals,

there are two types of melanin, the brownish black eumelanin and the reddish yellow pheomelanin. A suractivity of Tyr leads to overproduction of melanin leading to hyper-pigmentation of the skin. These phenomena have therefore encouraged researchers to study the activity of Tyr and to seek new potent inhibitors for use in cosmetics.

This review summarizes the different studies made on elastase, collagenase, hyaluronidase and tyrosinase by chromatographic (Table 1) and electrophoretic tools (Table 2). Analytical assays usually measure the product formation or the excess of substrate by separating the reaction mixture into its components. High performance liquid chromatography or HPLC and capillary electrophoresis or CE are the two main analytical techniques used for monitoring enzyme kinetics. The compatibility of these techniques with various detection modes (UV, DAD, LIF, C^4D and MS) makes them interesting for studying all types of molecules with low sample consumption, speed, automation of analysis and satisfactory sensitivity. The usefulness of HPLC and CE stems from their power as separation techniques and from their versatility.

2. Enzyme kinetics

a) Michaelis-Menten model

Enzymes are highly specific since they catalyze particularly a single chemical reaction or a set of closely related chemical reactions without the alteration of the equilibrium point of the reaction. When the reaction between an enzyme and its substrate occur, instead of a linear plot of velocity versus the substrate concentration, the experiment yields a hyperbolic curve. The analysis of the data suggested that the reaction is first-order at very low concentrations of substrate (S) and with the increase of S concentration ([S]), the reaction became progressively closer to zeroth-order. This phenomenon was explained by the fact that the enzyme and substrate interact to form an intermediate enzyme-substrate complex. The substrate binds to a very specific region of the enzyme molecule, called the active site that is highly active for specific substrates. The mechanism of enzyme catalyzed reactions is often studied by measuring rates of the enzyme-catalyzed reactions at different substrate and enzyme concentrations. The simplest model of an enzymatic reaction is:

$$E + S \underset{}{\overset{K_m^{app}}{\rightleftharpoons}} E - S \xrightarrow{k_{cat}} E + P \qquad \textbf{(1)}$$

Where E is the enzyme, S is the substrate, E-S the enzyme substrate complex and P the product of the enzyme-catalyzed reaction. K_m^{app} is the apparent Michaelis-Menten constant and k_{cat} is the catalytic constant or the turnover number of the forward reaction of E-S forming E + P.

The Michaelis-Menten equation presents the reaction velocity versus the substrate concentration. The Michaelis-Menten kinetics (K_m and V_{max}) can be determined by measuring velocity at a variety of substrate concentrations. These constants are observed when the entire enzyme present is fully saturated with substrate.

K_m is equal to the substrate concentration at which the reaction rate (v) is half its maximum value (V_{max}). The equation of the determination of Michaelis-Menten constant is:

$$v = \frac{V_{max}[S]}{K_m + [S]} \quad \textbf{(2)}$$

The value of K_m for an enzyme depends on the particular substrate, the pH of the incubation buffer (IB) and the temperature at which the reaction is carried out [31]. V_{max} is also related to k_{cat} by the equation:

$$k_{cat} = \frac{V_{max}}{[E]_T} \quad \textbf{(3)}$$

where $[E]_T$ corresponds to the total concentration of the enzyme.

b) Enzyme effectors

Many factors play an important role in the running of an enzymatic reaction (the ionic strength or salt concentration of the buffer, the presence of a major cation (Na^+, K^+) and pH). The optimal pH of an enzymatic activity depends also on the origin of the enzyme. Therefore, the human dermal fibroblast elastase has an optimum pH of 8.5 [32], the collagenase a pH of 7.4 [33], the hyaluronidase a pH of 3.7 [34] and the tyrosinase a pH of 6.4 [35]. The temperature plays also an important role for the activation of an enzymatic reaction [36]. Since the enzymes guide and regulate the metabolism of a cell and an organism, they tend to be controlled by regulatory molecules called effectors. These molecules can either increase or reduce enzyme's activity. Molecules that increase the activity are called activators, while those that decrease the activity are called inhibitors.

In order to determine the efficiency of an inhibitor/activator, a quantification of the effector potency is required. The two most common parameters for quantifying an effector are IC_{50} and k_i (the dissociation constant) for an inhibitor and AC_{50} and k_A (the activation constant) for an activator [37]. IC_{50} is the concentration of an inhibitor required to reduce the enzyme activity by 50% while AC_{50} is the concentration of an activator required to increase the enzyme activity by 50 %. A series of experiments are necessary to determine IC_{50} or AC_{50} value by maintaining a constant concentration of substrate so that the enzyme can react at an appreciable rate.

Activators or inhibitors can be natural, synthetic or semi-synthetic and are classified into two types: non-specific and specific [38, 39]. A non-specific inhibitor for example induces physical or chemical changes, which ultimately denatures the protein part of the enzyme and is therefore irreversible (pH, temperature, acids and bases).

The enzyme inhibition or activation can be either reversible or irreversible.

An irreversible reaction dissociates very slowly from its target enzyme because it has become tightly bound to the enzyme, either covalently or noncovalently. The reversible one, in contrast, is characterized by a rapid

dissociation of the enzyme-inhibitor/activator complex. A reversible reaction can be competitive, uncompetitive or non competitive. The competitive effector behaves such as the substrate and binds then to the active site of the enzyme. The substrate is thereby prevented from binding to the same active site. The following scheme represents a competitive inhibition:

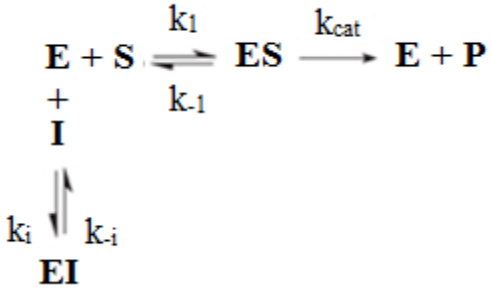

where $K_d = k_{-1}/k_1$ and $K_i = k_{-i}/k_i$; the classic expression is:

$$K_i = \frac{IC_{50}}{(S/K_m + 1)} \quad \textbf{(4)}$$

$$if \begin{cases} S = K_m \rightarrow K_i = IC_{50}/2 \\ S >> K_m \rightarrow K_i << IC_{50} \\ S << K_m \rightarrow K_i \cong IC_{50} \end{cases}$$

The uncompetitive inhibition occurs when the inhibitor binds to the enzyme-substrate complex and not to the free enzyme. In noncompetitive inhibition, the inhibitor and substrate can bind simultaneously to an enzyme molecule at different binding sites. The noncompetitive inhibition, in contrast with competitive inhibition, cannot be overcome by increasing the substrate concentration. A more complex pattern, called mixed inhibition, is produced when a single inhibitor both hinders the binding of substrate and decreases the turnover number of the enzyme.

Enzymatic reactions can be studied either by continuous assays, that give a continuous reading of activity, or by discontinuous assays, where samples are taken, the reaction is stopped and the concentrations of substrates and/or products are determined. The assay is the act of measuring how fast a given amount of enzyme will convert substrate to product by determining the velocity and requires the determination of the concentration of a product or substrate after a certain incubation time. Different methods can be used depending on the type of reaction catalyzed and the nature of substrate and product.

3. Chromatographic and electrophoretic tools for enzyme assays

In HPLC and CE, assays can be performed using two different modes (Figure 3). The first one, called offline mode, consists in mixing the enzyme and its substrate (in the presence or absence of the effector) outside the

separation column (or the capillary in CE). The pre-column assay is the most frequently used due to its simplicity. The enzymatic reaction occurs during a certain time of incubation in a vial containing an incubation buffer (IB). Then, a few nanolitres (1-10 nL) by CE or microliters (5-20 µL) by HPLC of the reaction mixture are injected in the separation column for analysis and quantification. For the reaction mixture, the enzyme may also be immobilized on silica particles or magnetic beads. In this case, the injection of the reactants can be done by continuous flow injection especially in HPLC. In the online mode, the separation column acts as an enzymatic nano- or micro- reactor and not only as a separation tool. Indeed, the enzymatic reaction takes place directly inside the column. In the heterogeneous mode, the enzyme (or occasionally the substrate) is immobilized inside the column. Moreover, multiple enzymes can be co-immobilized onto chromatographic supports. Reaction time can thus be shortened and fast screening of enzyme effectors can be performed. Immobilized enzymes generally maintain high catalytic specificity but may lose some of their catalytic efficiency. Their stability against heat, pH, and organic solvents is commonly increased by immobilization. However, the main problem in this process is related to the properties of support materials. The ideal support material should have good biocompatibility, known three-dimensional porous structure and chemical groups to avoid unspecific interactions with substrates and/or effectors. Many approaches for enzyme immobilization can be used depending on the properties of the target enzymes like entrapment, cross-linking, adsorption, or a combination of these methods [40]. In order to maintain the stability of the enzyme, covalent method is usually used to immobilize enzymes in the separation column [41].

Nowadays, capillary electrophoresis (CE) is one of the most promising analytical techniques for the study of enzymatic reactions [42-44]. Homogeneous assays can be used specifically in CE. In that case, all reactants - the enzyme, the substrate (and the inhibitor) - are free in solution and are introduced as separate plugs (plug-plug mode) in the capillary previously filled with the separation buffer also called the background electrolyte (BGE). A critical step of the successful development of such assays is to achieve an effective mixing of enzyme and substrate plugs into the capillary. For this, two main mixing modes have been employed based either on the electrophoretic migration or on the diffusion of the reactants inside the capillary. The first approach was introduced in 1992 by Bao and Regnier [45]. It is named electrophoretically mediated microanalysis or EMMA since it uses the different electrophoretic mobilities of the enzyme, substrate(s) and effector(s) for mixing reactants inside the capillary [44]. General parameters that have to be optimized for EMMA methods include reactant concentrations, plug lengths and injection sequence. The mixing by longitudinal diffusion of reactants through the interface between the plugs was named “at-inlet reaction” since the enzyme and the substrate plugs are placed at the inlet of the capillary. Another method called pressure-mediated microanalysis or PMMA was introduced in 2012 by our group [46] where mixing was obtained by longitudinal diffusion that is enhanced by applying a continuous pressure until detection. However, mixing using longitudinal diffusion is inefficient when relatively long plugs or more than two plugs are to be mixed because longitudinal diffusion is a rather

slow process. In order to overcome these limitations, mixing by transverse diffusion of laminar flow profiles (TDLFP) has been developed by Krylov et *al*. [47] in 2005 to assess β-galactosidase activity. This method is efficient for mixing two or more reactants inside a capillary. The injection of the reactants is conducted by applying relatively high pressure during short time to obtain plugs with a parabolic shape [47, 48] responsible for the mixing process by transverse diffusion [49]. Krylov et *al*. [50] also developed a software able to accurately simulate the spatial overlapping of plugs taking into account injection pressure, plug length, reactant coefficient of diffusion and concentration, and inner radius and length of the capillary.

More specifically, Tables 1 and 2 details the conditions optimized in literature for assaying elastase, collagenase, hyaluronidase and tyrosinase using chromatographic and electrophoretic approaches. These studies are detailed in the following sections.

4. Elastase activity monitored by HPLC, CE and microscale thermophoresis (MST)

The activity of elastase has been studied by several methods like photometry [51], nuclear magnetic resonance (NMR) [52], UV spectrophotometry [53], surface plasmon resonance [54] and also by chromatographic (Table 1) and electrophoretic (Table 2) tools as discussed below .

The first study of elastase by HPLC was done in 1989 by Stein et *al.* [55]. These authors developed a RPLC method to study the activity of elastase by measuring the quantity of elastin peptides obtained by the degradation of elastine. A simple offline assay was used to mix the enzyme with its natural substrate, the elastin. After 6, 24 and 48 h of incubation, the mixture was injected in a C_{18} column using a linear gradient from 0 to 10 % of 1-propanol containing 50 mM of heptafluorobutyric acid (pH 3.0). An online post column derivatization of the products obtained was then performed by mixing the mobile phase with 0.2 M of borate buffer (pH 8.0) followed by the addition of fluorescamine. More precisely, the dipeptide Val-Pro released was marked with the fluorescamine and followed for quantification at excitation and emission wavelengths of 395 and 455 nm, respectively. This method was also shown to be useful in the measurement of the elastolytic activity of tissues. However, the purification of the reaction mixture and the derivatization step were time- and reactant- consuming.

To facilitate the kinetic study of elastase, Viglio et *al.* [56] used short sequences of peptides that are representative of elastin. Three types of elastase were studied, human neutrophil elastase (HNE), *Aspergillus fumigatus* elastase, and porcine pancreatic elastase. Their appropriate substrates are presented in Table 1. An offline RPLC-based assay was developed based on the quantification of the released product (nitroaniline or NA) in each case. A C_{18} column was used and UV detection at 214 nm was conducted. Good linear regression was obtained and the K_m and V_{max} values evaluated were in good agreement with those obtained by conventional spectrometric assay at 410 nm. The aim of this work was also to develop a new approach by CE for the rapid determination of elastase activity, which could eventually become a promising alternative to the

spectrophotometric and HPLC-based techniques. Therefore, micellar electrokinetic chromatography (MEKC) was used to separate the products of the enzymatic reaction using 35 mM of tetraborate (pH 9.3) with 65 mM SDS and 15 % MeOH as running buffer. The peaks of the substrate and products were well resolved with a migration time of 15 min. K_m of MeO-Suc-Ala-Ala-Ala-Pro-Val-pNA (S_0) cleaved by HNE was successfully determined to be equal to 0.10 mM. These results were successfully comparable to those obtained by spectrophotometric and RPLC assays [56].

Using similar electrophoretic conditions, the same authors [57] analyzed the proteolytic activities of several elastases having different specificities of bond cleavage and present simultaneously in the incubation mixture. *Pseudomonas aeruginosa* elastase (PsE) and human leukocyte elastase (HNE) were incubated with Suc-Ala-Ala-Ala-NA (S_0) as substrate. PsE cleaves the substrate after the first alanine, giving then two products Suc-Ala-OH and Ala-Ala-NA while HNE gives Suc-Ala-Ala-Ala-OH and NA. The identification of all fragments obtained from the cleavage of the substrate by the two enzymes showed that MEKC was able to detect two different proteolytic activities simultaneously in a simple and efficient assay. K_m of PsE and of HNE were determined to be 0.67 and 4.5 mM, respectively. However, some limitations were present due to the use of SDS micelles, low detection sensitivity and relatively high reagent consumption (few tens of microliters).

Based on this work, our group studied the kinetics of HNE by developing new offline and online CE-based assays [58]. First of all, the short-end injection at the outlet side of the capillary was used in order to decrease the analysis time (3 min instead of 15 min) and the incubation buffer (25 mM HEPES and 20 mM NaCl) was optimized based on the "high salt stacking" method for a better sensitivity [59]. In these conditions, K_m for the substrate S_0 was determined to be 0.17 ± 0.04 mM and found to be similar to that determined by Viglio et *al*. [56] (Table 2). The consumption of analytes was minimized by using two online approaches based on EMMA and TDLFP for in-capillary mixing. With EMMA assay, the injection (~18 nL) sequence was conducted as follows: IB (incubation buffer), HNE, S_0 and IB. A plug of the IB was injected at the beginning of the injection sequence to prevent the inactivation of the enzyme by the background electrolyte or BGE (partial filling mode). A negative potential of -5 kV was then applied for 30 s across the capillary to electrophoretically mix the reactants (Table 2). The incubation time was only of 5 min and a voltage of - 25 kV was applied to separate the substrate from the products. For the determination of K_m and V_{max}, TDLFP was used. The injection sequence, presented in Figure 4.a, was therefore conducted in a sandwich mode to offer a good mixing of the enzyme with the substrate when the transversal diffusion will occur: IB, HNE, S_0, HNE (~7 nL) and then IB (~18 nL). The incubation time was also equal to 5 min and a voltage of -15 kV was applied for electrophoretic separation. This first IB plug must have a rectangular shape to avoid its transversal diffusion. K_m for S_0 was determined to be 0.13 ± 0.02 mM, which corresponds to the value obtained by offline MEKC assay (Figure 4.b). To increase the sensitivity of the developed assay, the laser induced fluorescence (LIF) detector was employed instead of UV and three synthetic peptides were tested as new potential substrates

for HNE by evaluating the corresponding catalytic constants; S_1 or 5-FAM-Ala-Ala-Ala-Val-OH, S_2 or 5-FAM-Ala-Ala-Ala-Phe-Tyr-Asp-OH and S_3 or 5-FAM-Arg-Glu-Ala-Val-Val-Tyr-OH. The tested substrates were chosen taking into account their ionization properties (pKa) to avoid the use of MEKC mode and the narrow cleavage site specificity of HNE. CZE-LIF used a 50 mM tetraborate buffer at pH 8.75 as BGE. Using TDLFP online assay, HNE was found to cleave S_2 and S_3 but failed with S_1 [60]. This was explained by the fact that HNE does not cleave the substrates containing in their structures the large hydrophobic amino acid Tyr in the position P'1 [61]. The catalytic constants of the two new substrates were successfully determined and the values showed good affinity (K_m = 0.07 mM) towards HNE compared to the reference substrate S_0 (K_m = 0.13 mM). The inhibition of HNE by two standard inhibitors from the triterpene family, the ursolic and the oleanolic acids, was assessed [60]. The solubility of the pentacyclic triterpenes was evaluated using two organic solvents, ethanol and DMSO. The effect of these solvent on HNE was monitored using a novel technique named microscale thermophoresis (MST) (Figure 5.a). This technique is based on the unique physical principle of thermophoresis, which is the directed motion of molecules in temperature gradients [62-64]. Under constant buffer conditions, thermophoresis probes the size, charge and hydration shell or conformation (solvation entropy) of the molecules. When ursolic acid was prepared in 5 % DMSO (v/v), a bumpy signal was observed on the thermophoretic curves indicating an aggregation of HNE. When stock solutions of ursolic acid were prepared in EtOH before their dilution in the IB, the aggregation of HNE was not observed as long as EtOH does not exceed 20 % (v/v). In these conditions, the K_i value for ursolic acid was equal to 2.72 ± 0.66 µM (Figure 5.b).IC_{50} values were also determined by online-CE assay using the following injection sequence: IB; HNE; inhibitor; S_3; inhibitor; HNE and IB (Table 2). The incubation time was 5 min. and the IC_{50} values were equal to 5.62 ± 0.10 µM for ursolic acid and 8.21 ± 0.23 µM for oleanolic acid. K_i values for ursolic and oleanolic acid, were deduced from Cheng-Prusoff equation as 2.81 ± 0.05 µM and 4.11 ± 0.12 µM, respectively. The LOQ of the CE-LIF assay was equal to 3 nM with no pre-concentration step.

To conclude, few studies were done for assaying elastase activity by offline based HPLC-assays. Offline and online based CE-assays were developed for the determination of kinetic constants (K_m, V_{max}, IC_{50} and K_i), and good repeatabilities, resolutions and sensitivities were obtained. In addition, the use of MST for the first time to study elastase-inhibitor interactions demonstrated it as powerful technique providing complementary information to CE and HPLC for monitoring enzyme-inhibitor affinity.

5. Collagenase activity monitored by HPLC and CE

HPLC was used for the first time to study vertebrate collagenase by Gray and Sanell in 1982 [65]. A simple offline assay was used to mix the collagenase present in *Rana catesbeiana tadpoles* with a synthetic substrate. A RPLC-UV method was developed to separate and quantify both the disappearance of the substrate 2,4-

dinitrophenyl-Pro-Gln-Gly-Ile-Ala-Gly-Gln-D-Arg and the appearance of the products 2,4-dinitrophenyl-Pro-Gln-Gly and Ile-Ala-Gly-Gln-D-Arg after collagenase cleavage. K_m and V_{max} were successfully determined to be 1.7 mM and 310 nmol.min^{-1}.mg^{-1}, respectively. Despite the efficiency of the assay, the method did not specify if substrate hydrolysis comes from the collagenase or other peptidases present in the skin of *Rana catesbeiana tadpoles*.

In 1988, Biondi et *al.* [66] studied the activity of bacterial collagenase using a synthetic peptide (Table 1). The product Gly-L-Pro-D-Arg obtained after collagenase hydrolysis was quantified by RPLC-UV using L-Pro-L-Phe as an internal standard. K_m and V_{max} were estimated to be 7.5 mM and 50.5 µmoles. min^{-1}.mg^{-1} with 0.2 µg of collagenase at pH 7.0 and 25°C. The reproducibility of the method was checked by analyzing 1 µg of collagenase and the resulting specific activity was 5.23 ± 0.27 U/mg with RSD of 5.2 % (n=5). This assay demonstrate that HPLC as a suitable technique to study collagenase activities. Using the same technique, the hydrolysis of dinitrophenyl-Pro-Gln-Gly-Ile_Ala-Gly-Gln-D-Arg by MMPs present in tissues around site of loose total hip arthroplasty prostheses was studied in 1996 [67]. A RPLC-UV was used for the quantification of the synthetic substrate. Results demonstrated that tissues extracted from periprosthetic total hip arthroplasty tissues presented elevated MMP activity (52.9 ± 19.7 %) compared with that in non-inflammatory synovial tissues from the knee joint (2.7 ± 61.9 %). After incubation with different antibiotics, MMP activity decreased significantly in the presence of cephalothin at 100 mg.mL^{-1} (31.9 ± 8.8 %) and 1000 mg.mL^{-1} (13.6 ± 0.1 %) in a dose-dependent manner. In addition, 500 µg of tetracycline inhibited MMP activity by 45.2 ± 8.5 %. However, doxycycline and gentamicin did not inhibit the MMP activity of the interface tissue extract. These findings conducted by HPLC show that cephalothin, a β-lactam antibiotic, can directly inhibit MMP activity in diseased human tissue when it is administered at therapeutically effective concentrations. Later on, Efsen et *al.* [68] developed an *in-vitro* offline assay to examine and quantify the proteolytic activity of MMPs in Crohn's disease fistulas specimens. Since different types of proteases exist in these fistulas, a specific fluorogenic substrate for MMP was used. Using HPLC with fluorescence detection, it was found that 50 % of the protease activity was ascribed to MMP activity and especially to MMP-3 and MMP-9. Furthermore, inhibition tests were done with ethylenediaminetetraacetic acid (EDTA), the synthetic broad-spectrum inhibitor GM6001, the angiotensin-converting enzyme inhibitor, ramiprilate, tetracycline, and doxycycline. Results have shown that ramiprilate decreased the total MMP activity level by 42 % and suppressed the specific MMP-3 activity by 72 %, which is comparable to the effect of GM6001 (87 %). Moreover, MMP-9 activity was completely blunted by ramiprilate. Doxycycline showed no effect on MMP activity, which corresponds with the findings cited previously [67]. The assay had good sensitivity and efficiency although the analysis lasted more than 30 min.

MMPs were studied by different offline and online CE-based assays as summarized in Table 2. In 1996, a simple preliminary study was done to separate collagen peptides derived from collagen type I using acid

buffers (pH 2.5) [69]. This separation was necessary before conducting any enzymatic reaction of collagenase by CE. Deyl el *al.* [70] used a pre-capillary assay where collagenase tissues were incubated with collagen type I according to the procedure described by Krane et *al*. [71]. The reaction was stopped by the addition of EDTA after 12 h. The mixture was injected by overpressure (3.5 kPa, 1s) and MEKC was used with a high concentration of surfactant. The analysis was carried out either in a 25 mM phosphate buffer (pH 2.5) or in a 25 mM phosphate buffer (pH 4.5) diluted to 0.1%, with respect to SDS. This study shows that when the separation is done in the straight mode at pH 2.5, the small peptides migrated faster than the larger ones with a shorter analysis time (roughly by a factor of three) compared to separations of collagen peptides which have come in contact with SDS during their preparation. When the separation was done at pH 4.5 with SDS, the larger peptides migrated ahead of the smaller ones. However, since the system must be run in the reversed polarity mode, the differences between the migration times of individual components were much higher and allowed an easy accumulation of the individual compounds in the anodic vial.

Miksik et *al*. [72] applied a model protein structure for detecting the nonenzymatic post-translational changes under various physiological conditions like high fructose diet and hypertriglyceridemic state. A mixture of collagen types I and III were incubated with bacterial collagenase then injected in CE using sodium phosphate buffer (pH 2.5). Almost 60 peaks of peptides were detected; however the origin of these peptides was unknown since no purification step was done. Principle component analysis (PCA) enabled to identify changes in the peptide profiles, allowing the determination of a section (part) of the electropherogram in which the physiological state changes occurred and was an excellent method for the analysis of these profiles. This approach was good to reveal which regime affects the collagen molecules most and can be used as guidance for targeted pre-separation of the very complex peptide mixture. Tosi et *al*. [73] used MEKC to study the activity of collagenase present in four species of *Arthrobotrys,* a genus of mitosporic fungi. Separations were performed using 50 mM sodium tetraborate, pH 9.3, containing 65 mM SDS and methanol (85/15, v/v). The calculated r^2 were ≥ 0.996 for the different products. Results showed that the total amount of collagenase produced by the Antarctic strain of *Arthrobotrys* tortor was about threefold higher than that observed for the other species. In the Antarctic strain, collagenase was shown to be a constitutive enzyme, which means it is produced in constant amounts regardless to the physiological demand or the concentration of the substrate.

In 2004, Sano et *al*. [74] developed a pre-capillary CE-LIF assay to study the effect of different inhibitors on three types of MMPs (-1, -8 and -13). These assays included the measurement of the activities of interstitial collagenase (MMP-1) and neutrophil collagenase (MMP-8) against type I collagen, and collagenase-3 (MMP-13) against type II collagen by determining the ¾ fragments produced after the cleavage. The mixture was injected in CE apparatus and the separation was done in 15 min using an electrolyte composed of 4 % of polyacrylamide and 0.05 % SDS (pH 8.8). The high sensitivity of the assays was achieved by employing NanoOrange, a non-covalent fluorescent dye for proteins. This method showed good repeatability and

sensitivity and was useful to estimate the IC_{50} values of three inhibitors: MMI-166, Metisam and BB-2516. It is therefore useful for proteinase assays since it enables conducting collagenase activity using native substrate without the need of antibody preparation. To improve the separation of the mixture of collagen peptides after a bacterial collagenase cleavage, Eckhardt et *al*. [75] added alkylamines, as dynamic coating agents, to the background phosphate buffer at pH 2.5. Ethylenediamine or 1,7-diaminoheptane used as background electrolyte modifiers improved the separation and yielded the best resolution. CZE was used in 2004 by Sheu et *al*. [76] to identify the presence of MMP-9 in human platelets and systematically examine its activity. To elucidate subcellular localization of MMP-9 in human platelets, intraplatelet MMP-9 was investigated by immunogold labeling and visualized using electron microscopy. Another way to separate a mixture of peptides consisted of a partial filling approach with combined gel and non-gel separation mechanisms in capillary electrophoresis [77]. In this work, a pre-capillary assay was used at high temperature with Pluronic F 127 as the gel matrix. Pluronic F was inserted as the first plug in the capillary, and the separation was done according to molecular weight and/or hydrophobicity. This method was applied firstly to the separation of a test peptide/protein mixture as well as on real samples containing peptides arising from collagen after collagenase cleavage and albumin after trypsin cleavage.

The first online CE-assay of MMPs was done in 2011 by Hai et *al*. [78]. This CE assay based on EMMA with LIF detection was used for the screening of MMP inhibitors. Two enzymes, MMP-2 and MMP-9, which have been considered as promising targets for cancer therapy, were selected as model enzymes. The hydrolysis of a fluorogenic substrate (Mca-Pro-Leu-Gly~Leu-Dpa-Ala-Arg-NH_2) catalyzed by MMPs was determined by measuring the increase in fluorescence. The enzyme was injected first, due to its lowest electrophoretic mobility. After the application of an electric field, the plugs of enzyme and then of the substrate and inhibitor mixture interpenetrated due to the differences in their apparent mobilities. The resultant reaction products as well as the unreacted substrate were electrophoretically transported toward the detector, where they were individually detected. In this study, the partial filling mode of EMMA was used (Figure 6.a). This establishes conditions under which inhibitors, regardless of charge, will mix with the enzyme when the mixing potential is applied. Compared with the normal-end injection at the inlet side of the capillary (Figure 6.b), short-end injection provided reduction in the analysis time to only 70 s, as well as an increase in peak sensitivity. Offline assay was also assessed in this study. K_m, V_{max} and IC_{50} of standard inhibitor (epigallocatechine gallate or EGCG) towards MMP-2 and MMP-9 were determined by offline and EMMA assays. To evaluate the screening potency of the developed assay, six known MMP inhibitors (oleanolic acid, caffeic acid, quercetin, doxycycline, resveratrol, and glucosamine) were tested on MMP-2 and MMP-9 by determining the inhibition percentage (I %). The comparison of the values with the offline assays indicated that EMMA with fluorescence detection is well suited for initial screening of a large number of compounds for MMP inhibition. For more sensitive and selective detection for MMP-9 study, mass spectrometry (MS) was coupled to CE by the same

group [79]. The advantage of in-capillary assay coupled with MS compared to fluorescence detection was that it allowed label free screening of enzyme inhibitors. Offline and online assays with MS detection were used for MMP-9 inhibitor screening. Different parameters were optimized for the coupling including sheath liquid flow rate, nebulizer pressure, dry gas flow temperature, and ESI voltage by two level half fractional experimental designs. The volatile buffer ammonium acetate (pH 6.8) was selected for both enzyme reaction and electrophoretic separation. Substrate and products were detected in only 5 min. After the optimization of different parameters (sheath liquid nature and flow, nebulizer pressure, drying gas flow, temperature and ESI voltage), the screening of five known inhibitors (GM6001, EGCG, doxycycline, minocycline, and tetracycline) and of four unknown inhibitors (chrysophanol, emodin, dioscin, and tetrahydropalmatine) was assessed. EMMA and PMMA were used for online incubation. The results demonstrated that the compound GM 6001 inhibited most of the activity of MMP-9. The I % of EGCG (~70 %) and doxycycline (~20 %) was consistent with the ones obtained in their previous study [78]. The RSDs on the peak area and the migration time of the product were 3.2 % and 3.9%, respectively for EMMA and 4.8 % and 0.9 %, respectively for PMMA. Good linearity was obtained in the tested range with $r^2 \geq 0.997$ for online assays. The LOD was equal to 10 nM for both methods.

In conclusion, different types of MMPs were studied by HPLC and CE-based assays. As for elastase, no immobilization was needed for collagenase study in HPLC. K_m, V_{max} and IC_{50} of different natural inhibitors were determined using both techniques. Online assays based on EMMA and PMMA were used for inhibitors screening; however TDLFP was not conducted. The use of LIF detection allowed better sensitivity and MS allowed selective detection and provided confirmation for all components within the reaction. Most of the applications mentioned in these studies were for therapeutic fields rather than for cosmetic ones, due to the important role of collagenases in tissue destruction.

6. Hyaluronidase activity monitored by HPLC and CE

The determination of Hyal activity involves the quantification of its ability to degrade HA. The increase in the number of sugar reducing ends was first monitored by simple chemical assays like calorimetry [80]. Benchetri et *al*. [81] used spectrophotometric assays to determine the amount of Hyal by measuring the interaction between undegraded HA and various dyes. Turbidity [82, 83], ELISA-like assay [84], agarose-gel electrophoresis [85], colorimetry [86] and zymography [87] can also be used.

In 1980, Knudsen et *al.* [88] followed by HPLC the products obtained after degradation of HA by bovine testicular hyaluronidase (BTH). This enzyme is commercially available and shows similar activity to human Hyal. An offline assay was used and the incubation was done for 120 h in order to reduce to the maximum the size of HA. After stopping the reaction by heating for 5 min, 20 µL of the mixture was injected into a C_{18}

column and the products were separated by size exclusion chromatography. HA was added to the mobile phase to prevent the adsorption of the products onto the column and for a better recovery. The chromatograms obtained showed the formation of tetra- and hexa- saccharide fractions and a low quantity of disaccharides. This method was efficient for the characterization of HA compound and of the enzymatic digestion products within 30 min of analysis time.

Later on, an HPLC method was developed to follow the quantity of HA present in synovial fluids [89]. Different incubation temperatures (4, 20 and 35 °C) with Hyal were tested. The temperature of 20 °C corresponded to the production of the highest quantity of tetra- and hexa- saccharide fractions. A reversed-phase octadecylsilyl column was used to separate the products of the Hyal reaction. An internal standard, the benzoic acid, was added to the mixture to improve precision. A good correlation factor ($r^2 = 0.99$) was found between HPLC and radiometry results. The separation of the main products tetra- and hexa- saccharides and the internal standard was done in almost 12 min with a good repeatability (CV ≤ 2.8 %; n=10). This method was suitable for direct determination of HA in synovial fluids and therefore as a biomarker.

Later on, Suzuki et *al.* [90] studied the inhibition of BTH by fully O-sulfated hyaluro-oligosaccharides using an amide-80 HPLC column and UV detection at 232 nm. The offline digestion was achieved in 48 h by determining the separation pattern of HAoligos that correspond to 40 % of digestion. CE was also used (Table 2). IC_{50} values of fully O-sulfated HA oligos were determined by HPLC with the flow injection assay method. Both CE and HPLC showed that each oligosaccharide ranged 4- to 20- mer was isolated with a purity higher than 90 %. The inhibitory action for Hyal of the oligosaccharides ranged 16- to 20- mer corresponded to 79 % through both competitive and noncompetitive effects.

In 2015, Kakizaki et *al.* [91] investigated the effects of HA oligosaccharides and chondroitin sulfates (CS) on BTH hydrolysis and transglycosylation activities. HA oligosaccharides corresponded to di-, tetra- and hexa-saccharide fractions while CS corresponded to tetra-, hexa-, octa- and even deca- saccharide fractions with a sulphatation of the position 4 or 6. More precisely, for the hydrolysis reaction, HA was used as a substrate and BTH was added in the presence or absence of HA and CS oligosaccharides at 37 °C for 1 h in acetate buffer (pH 5.0). These oligosaccharides were also tested in the presence of HA octasaccharide as a substrate. The products of this reaction were followed by HPLC with UV (215 nm) and fluorescence detection ($\lambda_{ex}/\lambda_{em}$ = 320/400 nm) using a polyamine II column (more details in Table 1). The chromatograms showed that HA oligosaccharides had no effect on BTH, while CS oligosaccharides inhibited its activity. In addition, results revealed that CS hexasaccharides or larger oligosaccharides inhibited BTH hydrolysis and transglycosylation more efficiently than CS tetrasaccharides. This is due to the increasing sulphate number improving the electrostatic interactions with the enzyme. Moreover, when the sulphation degree in the same chain is similar,

the inhibition of C4S (sulfate chondroitin in position 4) was shown to be greater than that of C6S oligosaccharide. In this study, the effect of homogeneous and heterogeneous sulphation was not assessed.

Aside from its presence in human skin, Hyal can also be found in animal venoms. Its presence increases the permeability of the tissues and accelerates therefore the spread of the venom. The determination of Hyal activity in snake and bee venom was done by CE in 1996 by Pattanaargson et *al*. [92] (Table 2). The method used was based on the addition of a quantity of HA to an aliquot of crude venom sample and then mixing during a fixed period of incubation. Hyal activity was measured by following the decrease in HA area due to its enzymatic hydrolysis. However, due to the complexity of Hyal mode of action, many authors [93-95] have observed that the degradation by Hyal of the products of HA hydrolysis also happens immediately after mixing of HA with Hyal. Their migration times may overlap with migration time of HA which makes the approach developed by Pattanaargson et *al.* inappropriate for quantitative analyses.

In 1997, Park et *al*. [96] studied the hydrolysis of HA by *Streptomyces hyaluronate lyase*. Since the products of this reaction are saccharide fractions with a similar charge density (a carboxylate group *per* disaccharide unit), their electrophoretic separation was difficult. These compounds have few chromophoric groups. Therefore, fluorescence detection was used to increase sensitivity after labeling with 7-amino 1,3-naphthalene disulfonic acid (AGA). The CE analysis required the use of a phosphate buffer of pH 2.3. Using this acidic pH, the AGA sulphonate group (pka <1) which is more acid than the carboxylate group of the saccharides (pka~3.5) becomes the only group responsible for the total charge of the oligosaccharides, ending up with a constant charge of -2 for each oligosaccharide. In this case, the electrophoretic separation of the HA oligosaccharides will only depend on their size. The formation of the various products of this enzymatic reaction was followed by detection of the fluorescence ($\lambda_{ex}/\lambda_{em}$ = 250/420 nm). Figure 7 shows that the electropherograms present a complicated mixture of oligosaccharides in the early reaction time. When the reaction is completed, only two major products are detected, the tetra- and hexa- saccharide fractions. This study demonstrated that Hyal acts on the HA according to an endolytic mechanism. Since only the labeled products are detected, the selectivity of this method makes possible the kinetic study of Hyal catalyzed reactions in more complex matrices.

HA depolymerization products were investigated by online CE-electrospray ionization-MS (CE/ESI-MS) for the first time in 2003 by Kuhn et *al*. [97]. The identification of several HA oligomers up to 16-mers was done using an ion trap mass spectrometer in less than 12 min. This coupling was shown to be promising for the qualitative analysis of negatively charged oligosaccharides. For the validation of this assay, extra experiments were conducted using gel-permeation chromatography (GPC) and viscosimetry [98]. Linear relationships were found between peak areas of the observed oligosaccharides and reaction times. To monitor the extent of degradation of HA by Hyal, the viscosity of HA fragments was measured. Indeed, the decrease in viscosity of the substrate solution corresponds to the number of cleavages of glycosidic bonds *per* time unit.

This coupling was later optimized by Grundmann et *al.* [99] using a CE-ESI-time-of-flight-MS (CE-ESI-TOF-MS) for the analysis of hyaluronan oligomer mixtures. An offline assay was performed with BTH (Table 2). The analytes showed best response in the negative ionization mode with an acidic sheath liquid (2-propanol/water/formic acid 50:50:0.2, v/v). Capillaries of 28 cm length and 15 µm i.d. were found to give best results. Optimal BGE contained 25 mM ammonium acetate (pH 8.5). CE-MS runs were completed in only 65 s which allowed a sample throughput of about 35 samples *per* hour.

Matysiak et *al.* [100] recently developed a new method for the determination of Hyal (from bovine testes and honeybee venom) activity using CZE with UV detection of the reaction products at 220 nm. A simple pre-capillary assay was used as shown in Table 2. Results showed that after 1.5 h of incubation, the products formed are tetra-, hexa- and octa- saccharide fractions. After increasing the incubation time to 24 h, disaccharide fractions appeared and octasaccharide fractions disappeared. A multiple regression analysis involving the heights of the peaks of the main HA degradation products was also performed. The method was validated by comparing the results with those obtained using pharmacopeia methods [101, 102].

The kinetic constants of Hyal were determined for the first time by CE-UV and CE-HRMS by our group [103]. A simple pre-capillary CE-UV/HRMS assay was used. Different parameters were studied to have the best sensitivity and are summarized in Table 2. The standard tetrasaccharide which is the final product of HA degradation by Hyal, was used For quantification. K_m and V_{max} were determined (n=3) using CE/UV at 200 nm as 0.24 ± 0.02 mg.mL^{-1} and 150.4 ± 0.1 nM.s^{-1}, respectively (Figure 8.a). They were also successfully obtained by CE/HRMS (n=3) with K_m of 0.49 ± 0.02 mg.mL^{-1} and V_{max} of 155.7 ± 0.2 nM.s^{-1} (Figure 8.a). IC_{50} of a standard natural inhibitor, EGCG, was also determined by CE-UV/HRMS (Figure 8.b). In addition, the activity of homemade tetrasaccharides of biotinylated chondroitin sulfate CS-A or CS-C (4- or 6- sulphated in a homogeneous or heterogeneous way) and of two trisaccharides from truncated linkage region of proteoglycans on the hydrolysis reaction of BTH was evaluated. Results showed that BTH was mostly dose-dependently inhibited by CS-A tetrasaccharides sulphated in a homogeneous way and that a small modification of one hydroxyl group changes the influence on BTH activity.

Later on, the previously developed CE-UV assay was used to screen the effect of extracts of a brown algae, *Padina pavonic*a, on BTH [104]. The extraction of this alga was optimized using several extraction techniques. A novel online CE-assay using TDLFP was developed allowing the efficient monitoring of BTH kinetics; K_m and V_{max} of 0.46 ± 0.04 mg.mL^{-1} and 137.1 ± 0.3 nM.s^{-1} (r^2=0.99; n=3), respectively. Figure 9 shows the electropherograms obtained with pressurized liquid ethyl acetate and water extracts. The water extract of *Padina pavonica* obtained by pressurized liquid extraction and microwave assisted extraction showed the highest anti-hyaluronidase activity (Figure 9). Therefore, its IC_{50} was determined by offline and online assays to be 25.2 ± 0.1 µg.mL^{-1} and 35.1 ± 0.1 µg.mL^{-1}, respectively.

To summarize, we can notice that different HPLC- and CE- methods were developed to study Hyal activity on HA. Various detectors were used to improve sensitivity and to identify the products obtained after HA cleavage. We can notice that BTH was mostly used to represent human Hyal activity. Compared to elastase and collagenase assays, the effect of a brown algae extracts were tested on hyaluronidase by offline and online CE-assays. These assays can be used for the screening of natural and synthetic inhibitors of Hyal activity for cosmetic and therapeutic applications.

7. Tyrosinase activity monitored by HPLC, HPTLC and CE

Tyr activity and inhibition was studied by many techniques such as UV/Vis spectroscopy [105]. In 1993, Shosuke Ito [106] developed an HPLC method to study the regulation of melanogenesis by analyzing quantitatively the contents of eu- and pheo- melanin in tissue samples without any purification procedure. Pyrrole-2,3,5-tri-carboxylic acid (PTCA) served as a quantitative indicator of eumelanin, whereas aminohydroxyphenylalanine (AHP) as a specific indicator of pheomelanin by UV absorbance at 254 nm. This method required 5 mg or less of tissue samples or 106 cultured cells for each analysis. The yields of PTCA and AHP were 2 % and 20 % from eu- and pheo- melanin, respectively. This study indicated that when Tyr activity is low, dopaquinone, a reactive intermediate in melanogenesis, is converted quantitatively to glutathionyldopa, which gives exclusively pheomelanin. However, when Tyr activity is high, an excess of dopaquinone is obtained, resulting in the inactivation of the essential enzymes for pheomelanogenesis. This method is very efficient since it has been successfully applied for the analysis of synthetic melanins, melanosomes, hair, feathers, melanomas, human epidermis and cultured melanocytes. In 2011, our group [107] developed a continuous-flow step gradient method for online kinetic tests of immobilized mushroom Tyr using MS for selective detection of product formation. This approach combined a continuous flow bioreactor and a frontal analysis chromatography (FAC) of ligand–Tyr binding methodology. FAC is an approach based on a LC-MS system enabling simultaneous ranking of the ligands/inhibitors according to their affinities to the biological target (enzyme/receptor). It involves the constant infusion of the studied ligand/inhibitor (or their mixture) and a non-interacting marker into the bioreactor with the immobilized target. Various flow rates of the mobile phase were tested, and in the different conditions, the values of K_m obtained were constant confirming the robustness of the developed assay. The use of MS allowed a selective monitoring of the enzymatic reaction products and for better sensitivity (500 pmol/min/column). K_i of kojic acid, a competitive inhibitor of Tyr, was determined for free and immobilized enzymes to be 3.56 ± 0.44 mM and 3.10 ± 0.05 mM, respectively. This method was automated. It allowed a simultaneous determination of specific inhibitor-Tyr interactions in complex mixtures and of k_i value of a given inhibitor. Later on, Yang et *al*. [108] developed a new assay based on ultrafiltration HPLC-DAD-MS^n for the rapid screening and identification of ligands for Tyr. This system is illustrated in Figure 10. The method was composed of three steps: incubation,

ultrafiltration, and characterization. The incubation process was designed to allow the sample solution to come into contact with the enzyme. Ethyl acetate extracts of mulberry leaves at 5 $mg.mL^{-1}$ were incubated with 160 µL of Tyr in 100 mM phosphate buffer (pH 6.8) at 25°C. Then, the unbound low-mass molecules were separated from the ligand–enzyme complexes by ultrafiltration after incubation for 30 min. The ultrafiltrates were injected directly into the HPLC–DAD–MS^n system for analysis. Tyr binding activity was determined by a decrease in peak areas of the detected chemicals corresponding to incubation with active Tyr. For comparison, control experiments with a denatured enzyme were also carried out which allowed to identify non-specific interactions. The identities of the "hits" were identified by online HPLC–DAD–MS^n analysis and by comparison with reference standards. Twelve compounds found in mulberry leaf extracts were characterized by HPLC-DAD-MS^n and two compounds, quercetin-3-O-(6-O-malonyl)-β-D-glucopyranoside and kaempferol-3-O-(6-O-malonyl)-β-D-glucopyranoside were identified as new Tyr inhibitors with an IC_{50} of 267.8 µM and 103.7 µM, respectively. The developed method was efficient for the screening and the identification of Tyr inhibitors in complex mixtures. The same approach was then used to identify inhibitors from *Xanthium strumarium* fruit extracts [109]. The false negatives were distinguished by optimizing the ultrafiltration-HPLC-DAD parameters to reduce the background noise and the false positives were distinguished by introducing a blocked Tyr in the control for comparison. Three competitive inhibitors 3,5-di-O-caffeoylquinic acid and 1,5-di-O-caffeoylquinic acid and one mixed-type inhibitor (chlorogenic acid) were identified in this study with IC_{50} of 1.07 ± 0.08 mM, 1.19 ± 0.03 mM and 1.05 ± 0.06 mM, respectively. O-caffeoylquinic acid and 1,5-di-O-caffeoylquinic acid were successfully distinguished as Tyr inhibitors from the false negatives and the false positives. Our group [110] studied again Tyr in 2014 using direct surface-assisted laser desorption/ionization (SALDI) and ESI-qTOF-MS. Mushroom Tyr was covalently coupled to core-shell-type silica-coated iron oxide magnetic nanoparticles (EMPs) that were applied as non-organic SALDI matrix suitable for studying low-mass compounds using a classic matrix-assisted laser desorption/ionisation time-of-flight (MALDI-TOF) mass spectrometer. The enzymatic conversion of glabridin and 3-(2,4-dihydroxyphenyl)propionic acid (DHPA) were also conducted by ESI-QqTOF-MS. This study showed that glabridin and DHPA were converted into the corresponding quinones by Tyr only in the presence of the auxiliary monophenol or o-diphenol substrates (L-Tyr and catechin, respectively) capable of regenerating the active site of Tyr. A post-TLC technique was developed in 2007 by Wangthong et *al.* [111] to make the isolation and purification of mushroom Tyr inhibitors easier and to differentiate between Tyr inhibitors and other components present in Licorice extract. A conventional TLC was used for a sample mixture containing octyl methoxy-cinnamate (not a Tyr inhibitor) and kojic acid (a standard Tyr inhibitor) as shown in Figure 11.a) and for arbutin and glabridin. The procedure consists of dropping the extract onto the bottom of the stationary phase and then to put the plate into 1:1 (v/v) hexane/ethylacetate as mobile phase. When the solvent front reached the mark, the plate was taken out and allowed to dry at room temperature.

Separated spots on the stationary phase were visualized and photographed under UV light. The entire plate was then sprayed with Tyr (0.02 mL/cm^2) and L-tyrosine (0.02 mL/cm^2) already prepared in 20 mM phosphate buffer (pH 6.8) to determine the presence of Tyr inhibitors in each spot. The different standard inhibitors gave a white spot whereas the spot obtained by octyl methoxy-cinnamate appeared as a dark background which validated the developed method. For Licorice extract, conventional two-dimensional TLC (2D-TLC) was used prior to the post chromatographic Tyr inhibitor detection (Figure 11.b). The first-dimensional TLC was carried out using 60:40 (v/v) methanol:dichloromethane as mobile phase and the second-dimensional separation was performed with 40:60 (v/v) hexane:ethyl acetate as a mobile phase. After complete TLC separation, one TLC plate was developed using the iodine absorption technique (used as a blank) while the other was sprayed with the Tyr and L-tyrosine. The TLC developed by Tyr/L-tyrosine spraying showed two active spots among six spots detected by iodine. This result confirmed the inhibitory effect of licorice extract on Tyr and the presence of at least two Tyr inhibitors with different polarities in the extract. This extract was then fractionated using a silica gel column eluted with 40:60 (v/v) hexane:ethyl acetate and the active fraction represented glabridin. These results show that the use of TLC provides valuable information for further isolation and purification of Tyr inhibitors from sample mixtures.

Later on, Momtaz et al. [112] studied the effect of three extracts (acetone, methanol and dichloromethane) of Sideroxylon inerme on Tyr and on melanocyte cells using the same previous procedure [111]. Results showed that methanol and acetone extracts presented an inhibition of 70%. However, no significant reduction was obtained with the dichloromethane extract at any of the tested concentrations. The methanolic extract was then fractionated with hexane, butanol and ethyl acetate. The ethyl acetate fraction exhibited the highest anti-tyr activity and the highest inhibition of melanin production in melanocyte cells (40 % at 25 and 50 µg/mL). EGCG and procyanidin were isolated from this fraction and their IC_{50} values were 30 µg/mL and 200 µg/mL, respectively. The referenced kojic acid and arbutin demonstrated IC_{50} values of 1.1 µg/mL and 149 µg/mL. The effect of the methanolic extract, EGCG, arbutin and kojic acid on cell viability and melanin production in B16F10 cells was also studied. Sideroxylon inerme extract showed a significant inhibition (37 %) of melanin production at 6.2 µg/mL while 80 % of cells were viable, thus indicating low levels of cytotoxicity. EGCG did not show any significant inhibition of melanogenesis at the different tested concentrations. Kojic acid (positive control) showed no significant toxicity to B16-F10 cells at the highest tested concentration and exhibited similar reduction in melanin content at 3.1 and 25 µg/mL (60 %). Compared with the positive controls (arbutin and kojic acid) and to procyanidin, EGCG exhibited more anti-Tyr activity than arbutin but less than kojic acid. These findings were very important for the identification of skin-depigmenting new agents. Kamagaju et *al.* [113] then evaluated *in-vitro* the ability of Rwandese medicinal plants and modulated Tyr activity. Therefore, five herbs (*Brillantaisia cicatricosa Lindau*, *Chenopodium ugandae*, *Dolichopentas longiflora Oliv.*, *Protea madiensis Oliv.* and *Sesamum angolense Welw*) were selected. Twenty-seven extracts, obtained

by treating the herbs with solvents of increasing polarities, were investigated for their effects on cell viability, on Tyr inhibition and on the measurement of melanogenesis by human melanoma cells. Results demonstrated that the tested plant extracts were not cytotoxic on human melanoma cell lines, except for *Dolichopentas longiflora*. All the extracts inhibited melanogenesis in melanoma cells. *Protea madiensis* extracts strongly inhibited melanogenesis and one of the *Dolichopentas longiflora* leaves extracts was found to increase melanogenesis. Crude cellular extracts obtained from normal melanocytes were used to confirm these results. The data obtained with the methanol extract of *Protea madiensis* were comparable when assaying on mushroom Tyr and on melanocyte proteins, while other extracts displayed discording data. This was due to the differences between human and mushroom Tyr, interference with melanocyte enzymes at later steps than Tyr or the simultaneous presence of compounds with conflicting activities in a given extract. This interesting study encourages authors to study the effect of extracts on the mushroom tyrosinase but also on the human one. In 2015, Taibon et *al.* [114] developed a simple and rapid HPTLC method to screen plant extracts for the presence of Tyr-inhibiting substances. Three different mobile phases were used for the separation of polar, nonpolar and very polar compounds. Several known Tyr inhibitors such as kojic acid, isoferulic acid, benzoic acid, resveratrol and tropolone were first tested as positive controls. The plates were first sprayed with *Levodopa* then with Tyr. The inhibitors should present white spots with white light in remission from the plate as well as with white light transmitted through the plate. However, some extracts included spots with different behaviors that may lead to false-positive results. This problem was eliminated by adding Triton X-100 to the *Levodopa* solution. The screening of thirteen extracts on one single HPTLC plate was possible in almost 90 min. The developed method was reproducible and suitable for the screening of plant extracts for Tyr without causing false-positive results. Additional information such as number or nature of active constituents was possible due to this technique after direct coupling with MS.

Chaita et *al.* [115] developed an integrated HPTLC-based methodology for the rapid tracing of the bioactive compounds from *Morus alba* extracts during bioassay-guided processes, using multivariate statistics. Two methodologies were therefore developed for the processing of the chromatograms; the assignment and the binning methodology. The first one consisted on the evaluation of the areas under curve of the analyzed peaks and the second one on applying the data binning technique. The multiple linear regression was chosen in order to have no correlations between the data and requiring more observations than variables. The conducted Tyr inhibition assays showed that oxyresveratrol, dihydrooxyresveratrol, transdihydromorin and 2,4,3'-trihydroxydihydrostilbene possess good inhibitory effect, with IC_{50} values 1.7 µM, 0.3 µM, 8.0 µM and 0.8 µM, respectively. Chemometric tools were shown in this study to support the development of a HPTLC-based methodology for the tracing of Tyr inhibitors in *Morus alba* extract and to afford essential key elements for application in high-throughput screening procedures for drug discovery purposes.

More recently, Boka et *al.* [116] aimed to combine high-throughput screening techniques (NMR, HPLC-based activity profiling and HPTLC-bioautography) in order to establish an integrated high-throughput multivariate statistics platform for the identification of natural products from *Paeonia mascula*, a greek plant. The extract of this plant was fractionated by fast centrifugal partition chromatography and the obtained fractions were then assayed for mushroom Tyr after analysis by HPTLC and NMR. HPTLC-bioautography permits the direct detection of the active compounds in the fractions, which leads to the target isolation. The use of NMR with multivariate statistics makes a direct structure elucidation possible. However, NMR is less sensitive compared to HPTLC and there is a possibility of false detection in case of similar variation of two or more compounds. Therefore, the combination of HPTLC and NMR employed with multivariate analysis, complemented each other providing a high-throughput platform for the discovery of natural products with skin whitening activity. In this study, eight active compounds were identified: 1,2,3,4,6-pentagalloyl glucopyranosid, gallic acid, gallic acid methyl ester and a mixture of meta and para digallic acid, quercetin-3-O-β-glucoside, kaempferol-3-O-β-glucoside-7-O-rhamnoside, 4′-methoxy quercetin 3-O-β-glucoside and kaempferol 3-O-β-glucoside.

CE was used in 1997 by Robinson and Smyth [117] to probe the biosynthesis of melanin for a better understanding of the processes involved in the oxidation of L-tyrosine and L-dopa. A simple pre-capillary assay was used where the intermediate products formed during L-tyrosine and L-dopa oxidation using Tyr were followed with DAD detection. In this work, an optimization of buffer preparations was done to maintain optimum working conditions of Tyr and 25 mM of tetraborate (pH 9.0) used as BGE facilitated rapid analyses. The CE-DAD technique was shown in this study to be useful for the analysis of intermediate compounds formed and for studies where sample volumes are limited.

The first online CE assay of Tyr was made in 2012 by Zhang et *al.* [118]. An EMMA-based CE assay was developed to screen Tyr inhibitors from traditional Chinese medicines. This method consisted of injecting a plug of the enzyme, followed by a plug of the substrate with or without the inhibitor. The activity of Tyr was detected by following the increase or decrease of quinine peak areas at 214 nm. The effect of the phosphate buffer concentration and of the incubation time was studied to optimize EMMA conditions. Best results were obtained with water as IB and 2 min of incubation time. K_m was determined to be 0.0532 mM and K_i of kojic acid was equal to 26.7 µM, which corresponds well to those previously obtained [107]. This method simplified the screening procedure by directly assaying the reaction product and minimized the false-positive effect.

To facilitate the study of Tyr, a chiral ligand exchange-CE (CLE-CE) was developed by Suna et *al.* [119]. This system employs Zn (II)-L-Alanine complex as a chiral ligand for quantitative analysis of dansylated L-amino acids. It investigates the activity of Tyr through monitoring the L-tyrosine concentration. Before conducting the reaction, the separation conditions were optimized with 100 mM boric acid, 5 mM ammonium acetate, 4 mM Zn (II), 8 mM L-Ala and 4 mM β-CD at pH 8.2. Under these conditions and using pre-capillary approach, K_m and V_{max} were determined to be 374 µM and 172 µM.min^{-1}, respectively. This method was also used to

study the effect of kojic acid and of soy sauce. For the screening of another family of Tyr inhibitors, the chalcones, the authors optimized CLE-CE method by replacing the chiral ligand by L-leucine [120]. Despite the good separation of dansylated-D-L-amino acids, the migration time was above 50 min.

In 2013, a heterogeneous assay based on the immobilization of Tyr was developed by Jiang et *al.* [121] (Figure 12). Tyr was immobilized on the surface of fused-silica-capillary by ionic binding with the cationic polyelectrolyte hexadimethrien bromide (HDB). The HDB solution (0.1 %) was first injected into the capillary and kept for 5 min to create a positively charged coating on the capillary wall. This injection was followed by a plug of the enzyme (50 mbar for 10 s) at a concentration of 0.5 $mg.mL^{-1}$. Another plug of HDB solution (0.1 %) was then injected to cover the immobilized enzyme. For activity and inhibition assays, the capillary was first filled with a BGE of 20 mM phosphate and 0.01 % HDB at pH 7.4, followed by a plug of L-tyrosine with or without the inhibitor at 50 mbar for 10 s. An illustration of this layer-by-layer assembly is shown in Figure 12. Enzyme activities were quantified by following the decrease or the increase of peak areas of DOPA in the presence or absence of inhibitors. The K_m value was determined to be 0.053 mM and the K_i of kojic acid was equal to 24.54 µM, which is comparable to the work of Zhang et *al.* [118] using EMMA. The inhibitory ratios of enzymatic activity of traditional Chinese medicine were established. *Fructus crataegi* and *Radix angelicae pubescentis* inhibited Tyr by 62 % and 65 %, respectively. These values were also comparable with those obtained by Zhang et *al.* [118].

A new method based on Tyr immobilization was developed recently by Cheng et *al.* [122]. This reliable online immobilization enzyme microreactor (IMER) was constructed at the outlet of the capillary by using glutaraldehyde as cross-linker. The short-end injection was used. The substrate and product were separated within only 2 min. Immobilization prolonged the storage of the enzyme where immobilized Tyr remained 80 % active for 30 days at 4°C. Fifteen natural compounds from traditional Chinese medicine were screened using this method and quercetin and kaempferol were shown to have good inhibitory potency, of 34.7 ± 3.1 % and 24.2 ± 4.3 %, respectively. In addition, molecular docking was carried out to demonstrate the inhibitory potential of quercetin, kaempferol, bakuchiol and bavachinin.

From these studies, it can be concluded that immobilization assays were more often used for assaying Tyr activity in the absence or in the presence of different inhibitors. Several on-line assays were conducted. For online CE-assays, EMMA was the only method used. K_m, V_{max} and IC_{50} of different natural molecules were also determined. It should also be noted that the study on real cells was also presented in the cited studies which is of great importance in many applications.

8. Limitations and future development

As shown in this review, there has been a reasonable amount of papers dealing with the use of chromatographic and electrophoretic tools for studying elastase, collagenase, hyaluronidase, and tyrosinase kinetics. Continuous

innovation in micro- and nano- fluidic research and promising multiplexing of microchip formats revealed significant potentials in coupling high-throughput to miniaturization of biochemical assays for broader usage and developments in the cosmetic and the therapeutic fields. For this, further miniaturization by using microchips hyphenated to mass spectrometry can be very interesting. Moreover, for more accuracy it will be essential to use these techniques to evaluate enzymatic activity directly in whole cells (as noticed by Kamagaju et al. [124]). Our group has already showed that cell membranes can be disrupted in-capillary by electroporation and that the released enzymes can be subsequently studied and quantified in the same capillary [44] by monitoring the formed products.

9. Conclusion

The examples referenced above confirm that HPLC, HPTLC, CE as well as the more recent MST were efficiently used for studying elastase, collagenase, hyaluronidase and tyrosinase. Assays were conducted for the screening of natural or synthetic inhibitors of these enzymes and for applications on cells such as keratinocytes, fibroblasts and melanocytes. Offline mode in CE and HPLC was the most frequently used since it is easy to optimize and to perform. The speed of analysis and minimal sample consumption are the main advantages of these analytical tools. The versatile use of different types of detectors with no limits imposed by radiolabeling pushed these techniques further and further beyond their limits, encouraging their use by scientists all over the world for enzymatic assays.

Acknowledgments

Authors would like to thank the Region Centre (France) for its financial support (research project PODOUCE, APR 2014).

The authors declare that there are no conflicts of interest.

References

[1] B. Marte, J. Finkelstein, L. Anson, Nature insight: skin biology, Nat. Biotechnol. 445 (2007) 833-880.

[2] P. Olczyk, Ł. Mencner, K. Komosinska-Vassev, The role of the extracellular matrix components in cutaneous wound healing, BioMed. Res. Int. 2014 (2014) 1-8.

[3] J. K. Mouw, G. Ou, V. M. Weaver, Extracellular matrix assembly: a multiscale deconstruction, Nat. Rev. Mol. Cell Biol. 15 (2014) 771-785.

[4] M. A. Farage, K. W. Miller, P. Elsner, H. I. Maibach, Intrinsic and extrinsic factors in skin ageing: a review, Int. J. Cosmetic Sci. 30 (2008) 87-95.

[5] M. A. Farage, K. W. Miller, P. Elsner, H. I. Maibach, Structural characteristics of the aging skin, Cutan. Ocul. Toxicol. 26 (2007) 343-357.

[6] J. S. Koh, H. Kang, S. W. Choi, H. O. Kim, Cigarette smoking associated with premature facial wrinkling: image analysis of facial skin replicas, Int. J. Dermatol. 41 (2002) 21-27.

[7] K. E. Kim, D. Cho, H. J. Park, Air pollution and skin diseases: Adverse effects of airborne particulate matter on various skin diseases, Life Sci. 152 (2016) 126-134.

[8] F. González-Illán, G. Ojeda-Torres, L. M. Díaz-Vázquez, O. Rosario, Detection of fatty acid ethyl esters in skin surface lipids as biomarkers of ethanol consumption in alcoholics, social drinkers, light drinkers, and teetotalers using a methodology based on microwave assisted extraction followed by solid phase microextraction and gas chromatography- mass spectrometry, J. Anal. Toxicol. 35 (2011) 232-237.

[9] K. H. Al-Gubory, Environmental pollutants and lifestyle factors induce oxidative stress and poor prenatal development, Reprod. BioMed. Online 29 (2014) 17-31.

[10] R. Zhai, Y. Zhao, G. Liu, M. Ter-Minassian, I.-C. Wu, Z. Wang, L. Su, K. Asomaning, F. Chen, M. H. Kulke, X. Lin, R. S. Heist, J. C. Wain, D. C. Christiani, Interactions between environmental factors and polymorphisms in angiogenesis pathway genes in esophageal adenocarcinoma risk: a case-only study, Cancer 118 (2012) 804-811.

[11] M. Ushio-Fukai, Y. Nakamura, Reactive oxygen species and angiogenesis: NADPH oxidase as target for cancer therapy, Cancer Lett. 266 (2008) 37-52.

[12] I. F. d. S. Videira, D. F. L. Moura, S. Magina, Mechanisms regulating melanogenesis, An. Bras. Dermatol. 88 (2013) 76-83.

[13] T. Chiba, H. Uchi, G. Tsuji, H. Gondo, Y. Moroi, M. Furue, Arylhydrocarbon receptor (AhR) activation in airway epithelial cells induces MUC5AC via reactive oxygen species (ROS) production, Pulm. Pharmacol. Ther. 24 (2011) 133-140.

[14] B. A. Gilchrest, H.-Y. Park, M. S. Eller, M. Yaar, Mechanisms of ultraviolet light-Iinduced pigmentation, Photochem. Photobiol. 63 (1996) 1-10.

[15] N. Furnham, I. Sillitoe, G. L. Holliday, A. L. Cuff, R. A. Laskowski, C. A. Orengo, J. M. Thornton, Exploring the evolution of novel enzyme functions within structurally defined protein superfamilies, Plos 8 (2012) 1-13.

[16] P. Imming, C. Sinning, A. Meyer, Drugs, their targets and the nature and number of drug targets, Nature 5 (2006) 821-834.

[17] N. Tsuji, S. Moriwaki, Y. Suzuki, Y. Takema, G. Imokawa, The role of elastases secreted by fibroblasts in wrinkle formation: implication through selective inhibition of elastase activity, Br. J. Dermatol. 74 (2001) 283-290.

[18] Y. Li, W. Xia, Y. Liu, H. A. Remmer, J. Voorhees, G. J. Fisher, Solar ultraviolet irradiation induces decorin degradation in human skin likely via neutrophil elastase, Plos one 8 (2013) e72563.

[19] N. Morisaki, S. Moriwaki, Y. Sugiyama-Nakagiri, K. Haketa, Y. Takema, G. Imokawa, Neprilysin is identical to Skin Fibroblast Elastase, J. Biol. Chem. 285 (2010) 39819-39827.

[20] O. B. G. Jr, M. Febbraio, R. Simantov, R. Zheng, R. Shen, R. L. Silverstein, D. M. Nanus, Neprilysin Inhibits Angiogenesis via Proteolysis of Fibroblast Growth Factor-2, J. Biol. Chem. 281 (2006) 33597–33605.

[21] N. Philips, M. Samuel, R. Arena, Y.-J. Chen, J. Conte, P. Natrajan, G. Haas, S. Gonzalez, Direct inhibition of elastase and matrix metalloproteinases and stimulation of biosynthesis of fibrillar collagens, elastin, and fibrillis by xanthohumol, J. Cosmetic Sci. 61 (2010) 125-132.

[22] O. Wiedow, F. Wiese, E. Christophers, Lesional elastase activity in psoriasis. Diagnostic and prognostic significance, Arch. Dermatol. Res. 287 (1995) 632-635.

[23] J. Ray, W. Stetler-Stevenson, The role of matrix metalloproteases and their inhibitors in tumour invasion, metastasis and angiogenesis, Eur. Respir. J. 7 (1994) 2062-2072.
[24] I. Mikšík, P. Sedlákováa, K. Mikulíkováa, A. Eckhardta, Capillary electromigration methods for the study of collagen, J. Chromatogr. B 841 (2006) 3-13.
[25] J. Necas, L. Bartosikova, P. Brauner, J. Kolar, Hyaluronic acid (hyaluronan): a review, Vet. Med. 8 (2008) 397-411.
[26] E. Papakonstantinou, M. Roth, G. Karakiulakis, Hyaluronic acid: A key molecule in skin aging, Dermatoendocrinol. 4 (2012) 253-258.
[27] R. Stern, M. J. Jedrzejas, Hyaluronidases: their genomics, structures, and mechanisms of action, Chem. Rev. 106 (2006) 818-839.
[28] W. Knudson, M. W. Gundlach, T. M. Schmid, H. E. Conrad, Selective hydrolysis of chondroitin sulfates by hyaluronidase, Biochem. 23 (1984) 368-375.
[29] P. Hoffman, K. Meyer, A. Linker, Transglycosylation during the mixed digestion of hyaluronic acid and chondroitin sulfate by testicular hyaluronidase, J. Biol. Chem. 219 (1955) 653-663.
[30] R. Stern, M. J. Jedrzejas, The hyaluronidases: their genomics, structures, and mechanisms of action, Chem. Rev. 106 (2008) 818-839.
[31] H. Bisswanger, Enzyme assays, Perspect. Sci. 1 (2014) 41-55.
[32] A. J. Barrett, Leukocyte elastase, Method Enzymol. 80 (1981) 581-588.
[33] J. Varani, D. Spearman, P. Perone, S. E. G. Fligiel, S. C. Datta, Z. Q. Wang, Y. Shao, S. Kang, G. J. Fisher, J. J. Voorhees, Inhibition of type I procollagen synthesis by damaged collagen in photoaged skin and by collagenase-degraded collagen in vitro, Am. J. Pathol. 158 (2001) 931-942.
[34] S. Stair-Nawy, A. B. Csoka, R. Stern, Hyaluronidase expression in human skin fibroblasts, Biochem. Biophys. Res. Commun. 266 (1999) 268-273.
[35] F. Garcia-Molina, A. N. P. Hiner, L. G. Fenoll, J. N. Rodriguez-Lopez, P. A. Garcia-Ruiz, F. Garcia-Canovas, J. Tudela, Mushroom tyrosinase: catalase activity, inhibition, and suicide inactivation, J. Agric. Food Chem. 53 (2005) 3702−3709.
[36] N. Tamanna, N. Mahmood, Food processing and Maillard reaction products: effect on human health and nutrition, Int. J. Food Sci. 2015 (2015) 1-6.
[37] M. Potier, S. Giroux, Regulatory proteins (inhibitors or activators) affect estimates of M_r of enzymes and receptors by radiation inactivation, Biochem. J. 226 (1985) 797-801.
[38] W.-Y. Ong, T. Farooqui, G. Kokotos, A. A. Farooqui, Synthetic and natural inhibitors of phospholipases A2: their importance for understanding and treatment of neurological disorders, ACS Chem. Neurosc. 6 (2015) 814-831.
[39] S. Y. Lee, N. Baek, T.-g. Nam, Natural, semisynthetic and synthetic tyrosinase inhibitors, J. Enzyme Inhib. Med. Chem. 31 (2016) 1.
[40] S.-M. Fang, H.-N. Wang, Z.-X. Zhao, W.-H. Wang, Immobilized enzyme reactors in HPLC and its application in inhibitor screening: a review, J. Pharm. Anal. 2 (2012) 83-89.
[41] J. J. Bao, J. M. Fujima, N. D. Danielson, Determination of minute enzymatic activities by means of capillary electrophoretic techniques, J. Chromatogr. B 699 (1997) 481-497.
[42] R. Nehmé, P. Morin, Advances in capillary electrophoresis for miniaturizing assays on kinase enzymes for drug discovery, Electrophoresis 36 (2015) 2768-2797.
[43] Y. Fan, G. K. E. Scriba, Advances in-capillary electrophoretic enzyme assays, J. Pharm. Biomed. Analysis 53 (2010) 1076-1090.
[44] H. Nehmé, R. Nehmé, P. Lafite, E. Duverger, S. Routier, P. Morin, Electrophoretically mediated microanalysis for in-capillaryelectrical cell lysis and fast enzyme quantification by capillary electrophoresis, Anal. Bioanal. Chem. 405 (2013) 9159-9167.
[45] J. Bao, F. E. Regnier, Ultramicro enzyme assays in a capillary electrophoretic system, J. Chromatogr. A 608 (1992) 217-224.
[46] H. Nehmé, R. Nehmé, P. Lafite, S. Routier, P. Morin, New development in in-capillary electrophoresis techniques for kinetic and inhibition study of enzymes, Anal. Chim. Acta 722 (2012) 127–135.
[47] V. Okhonin, X. Liu, S. N. Krylov, Transverse diffusion of laminar flow profiles to produce nanoreactors, Anal. Chem. 77 (2005) 5925-5929.

[48] H. Nehmé, R. Nehmé, P. Lafite, S. Routier, P. Morin, Human protein kinase inhibitor screening by capillary electrophoresis using transverse diffusion of laminar flow profiles for reactant mixing, J. Chromatogr. A 1314 (2013) 298-305.
[49] V. Okhonin, A. P. Petrov, S. M. Krylova, S. N. Krylov, Quantitative characterization of micromixing based on uniformity and overlap, Angew. Chem. Int. Ed. 50 (2011) 11999-12002.
[50] S. M. Krylova, V. Okhonin, C. J. Evenhuis, S. N. Krylov, The inject-mix-react-separate-and-quantitate (IMReSQ) approach to studying reactions in capillaries, Trend. Anal. Chem. 28 (2009) 987-1010.
[51] A. Hasmann, U. Gewessler, E. Hulla, K. P. Schneider, B. Binder, A. Francesko, T. Tzanov, M. Schintler, J. V. d. Palen, G. M. Guebitz, E. Wehrschuetz-Sig, Sensor materials for the detection of human neutrophil elastase and cathepsin G activity in wound fluid, Exp. Dermat. 20 (2011) 508-513.
[52] V. Mansuy-Aubert, Q. L. Zhou, X. Xie, Z. Gong, J.-Y. Huang, A. R. Khan, G. Aubert, K. Candelaria, S. Thomas, D.-J. Shin, S. Booth, S. M. Baig, A. Bilal, D. Hwang, H. Zhang, R. Lovell-Badge, S. R. Smith, F. R. Awan, Z. Y. Jiang, Imbalance between neutrophil elastase and its inhibitor α1-antitrypsin in obesity alters insulin sensitivity, inflammation, and energy expenditure, Cell Metab. 17 (2013) 534-548.
[53] R. L. Stein, Catalysis by human leukocyte elastase: substrate structural dependence of rate-limiting protolytic catalysis and operation of the charge relay system, J. Am. Chem. Soc. 105 (1983) 5111–5116.
[54] B. Shen, S. Shimmon, M. M. Smith, P. Ghosh, Biosensor analysis of the molecular interactions of pentosan polysulfate and of sulfated glycosaminoglycans with immobilized elastase, hyaluronidase and lysozyme using surface plasmon resonance (SPR) technology, J. Pharm. Biomed. Anal. 31 (2003) 83-93.
[55] T. A. Stein, J. R. Cohen, C. Mandell, L. Wise, Determination of elastase activity by reversed-phase high-performance liquid chromatography, J. Chromatogr. 461 (1989) 267-270.
[56] S. Viglio, G. Zanaboni, M. Luisetti, G. Cetta, M. Guglielminetti, P. Iadarola, Micellar electrokinetic chromatography: A convenient alternative to colorimetric and high performance liquid chromatographic detection to monitor protease activity, Electrophoresis 19 (1998) 2083-2089.
[57] S. Viglio, M. Luisetti, G. Zanaboni, G. Doring, D. Worlitzsch, G. Cetta, P. Iadarola, Simultaneous determination of Pseudomonas aeruginosa elastase, human leukocyte elastase and cathepsin G activities by micellar electrokinetic chromatography, J. Chromatogr. A 846 (1999) 125-134.
[58] S. Fayad, R. Nehmé, P. Lafite, P. Morin, Assaying Human Neutrophil Elastase activity by capillary zone electrophoresis combined with laser-induced fluorescence (CZE-LIF), J. Chromatogr. A 1419 (2015) 116-124.
[59] J. F. Palmer, High-salt stacking principles and sweeping: comments and contrasts on mechanisms for high-sensitivity analysis in capillary electrophoresis, J. Chromatogr. A 1036 (2004) 95-100.
[60] S. Fayad, R. Nehmé, B. Claude, P. Morin, Human neutrophil elastase inhibition studied by capillary electrophoresis with laser induced fluorescence detection (LIF) and microscale thermophoresis (MST), J. Chromatogr. A 1431 (2016) 215–223.
[61] W. Bode, E. M. Jr, O. B. Goodman, J. C. Powers, Human leukocyte and porcine pancreatic elastase: X-ray crystal structures, mechanism, substrate specificity, and mechanism-based inhibitors, Biochem. 28 (1989) 1951-1963.
[62] M. Jerabek-Willemsen, C. J. Wienken, D. Braun, P. Baaske, S. Duhr, Molecular interaction studies using microscale thermophoresis, Assay Drug Dev. Technol. 9 (2011) 342-353.
[63] M. Jerabek-Willemsen, T. André, R. Wanner, H. M. Roth, S. Duhr, P. Baaske, D. Breitsprecher, MicroScale Thermophoresis: Interaction analysis and beyond, J. Mol. Structure 1077 (2014) 101-113.
[64] S. A. I. Seidel, P. M. Dijkman, W. A. Lea, G. v. d. Bogaart, M. Jerabek-Willemsen, A. Lazic, J. S. Joseph, P. Srinivasan, P. Baaske, A. Simeonov, I. Katritch, F. A. Melo, J. E. Ladbury, G. Schreiber, A. Watts, D. Braun, S. Duhr, Microscale thermophoresis quantifies biomolecular interactions under previously challenging conditions, Meth. 59 (2013) 301–315.
[65] R. D. Gray, H. H. Saneii, Characterization of vertebrate collagenase activity by high-performance liquid chromatography using a synthetic substrate, Anal. Biochem. 120 (1982) 339-346.
[66] P. A. Biondi, F. Manca, A. Negri, A. Berrini, T. Simonic, C. Secchi, High-performance liquid chromatographic assay of bacterial collagenase, Chromatographia 25 (1988) 659-662.
[67] S. Santavirta, M. Takagi, Y. T. Konttinen, T. Sorsa, A. Suda, Inhibitory effect of cephalothin on matrix metalloproteinase activity around loose hip prostheses, Antimicrob. Agents Chemother. 40 (1996) 244-246.

[68] E. Efsen, T. Særmark, A. Hansen, E. Bruun, J. Brynskov, Ramiprilate inhibits functional matrix metalloproteinase activity in Crohn's disease fistulas, Basic. Clin. Pharmacol. Toxicol. 109 (2011) 208-216.
[69] J. Novotná, Z. Deyl, L. Miksík, Capillary zone electrophoresis of collagen type I CNBr peptides in acid buffers, J. Chromatogr. B 681 (1996) 77-82.
[70] Z. Deyl, J. Novotna, I. Miksık, J. Herge, Micropreparation of tissue collagenase fragments of type I collagen in the form of surfactant–peptide complexes and their identification by capillary electrophoresis and partial sequencing, J. Chromatogr. A 796 (1998) 181-193.
[71] S. M. Krane, M. H. Byrne, V. Lemaître, P. Henriet, J. J. Jeffrey, J. P. Witter, X. Liu, H. Wu, R. Jaenisch, Y. Eeckhout, Different collagenase gene products have different roles in degradation of type I collagen, J. Biol. Chem. 271 (1996) 28509-28515.
[72] I. Miksık, A. Eckhardt, T. Cserhati, E. Forgacs, J. Zicha, Z. Deyl, Evaluation of peptide electropherograms by multivariate mathematical–statistical methods I. Principal component analysis, J. Chromatogr. A 921 (2001) 81-91.
[73] S. Tosi, L. Annovazzi, IlariaTosi, P. Iadarola, G. Caretta, Collagenase production in an antarctic strain of arthrobotrys tortor jarowaja, Mycopathol. 153 (2001) 157-162.
[74] M. Sano, I. Nishino, K. Ueno, H. Kamimori, Assay of collagenase activity for native triple-helical collagen using capillary gel electrophoresis with laser-induced fluorescence detection, J. Chromatogr. B 809 (2004) 251–256.
[75] A. Eckhardt, I. Mikšík, Z. Deyl, J. Charvátová, Separation of low-molecular mass peptides by capillary electrophoresis with the use of alkylamines as dynamic coating agents at low pH, J. Chromatogr. A 1051 (2004) 111-117.
[76] J. R. Sheu, T. H. Fong, C. M. Liu, M. Y. Shen, T. L. Chen, Y. Chang, M. S. Lu, G. Hsiao, Expression of matrix metalloproteinase-9 in human platelets: regulation of platelet activation in in vitro and in vivo studies, Br. J. Pharmacol. 143 (2004) 193-201.
[77] P. Sedlakova, J. Svobodova, I. Miksik, Capillary electrophoresis of peptides and proteins with plug of Pluronic gel, J. Chromatog. B 839 (2006) 112-117.
[78] X. Hai, X. Wang, M. El-Attug, E. Adams, J. Hoogmartens, A. V. Schepdael, In-Capillary screening of matrix metalloproteinase inhibitors by electrophoretically mediated microanalysis with fluorescence detection, Anal. Chem. 83 (2011) 425-430.
[79] X. Wang, Z. Dou, Y. Yuan, S. Mand, K. Wolfs, E. Adams, A. V. Schepdael, On-line screening of matrix metalloproteinase inhibitors by capillary electrophoresis coupled to ESI mass spectrometry, J. Chromatog. B 930 (2013) 48-53.
[80] N. D. Ferrante, Turbidimetric measurement of acid mucopolysaccharides and hyaluronidase activity, J. Biol. Chem. 220 (1956) 303-306.
[81] L. C. Benchetrit, S. L. Pahuja, E. D. Gray, R. D. Edstrom, A sensitive method for the assay of hyaluronidase activity, Anal. Biochem. 79 (1977) 431-437.
[82] N. D. Ferranre, Turbidimetric measurement of acid mucopolysaccharides and hyaluronidase activity, J. Biol. Chem. 220 (1956) 303-306.
[83] J. Bhavya, M. S. Vineetha, P. M. Sundaram, S. M. Veena, B. L. Dhananjaya, S. S. More, Low-molecular weight hyaluronidase from the venom of Bungarus caeruleus (Indian common Krait) snake: Isolation and partial characterization, J. Liq. Chromatogr. Relat. Technol. 39 (2016) 203-208.
[84] M. Stern, R. Stern, An ELISA-like assay for hyaluronidase and hyaluronidase inhibitors, Matrix 12 (1992) 397-403.
[85] J. Müllegger, S. Reitinger, G. Lepperdinger, Hapten-labeled hyaluronan, a substrate to monitor hyaluronidase activity by enhanced chemiluminescence-assisted detection on filter blots, Anal. Biochem. 293 (2001) 291-293.
[86] W. M. B. Jr., E. Y. Cantey, Colorimetric method for determination of serum hyaluronidase activity, Clin. Chim. Acta 13 (1966) 746-752.
[87] M. W. Guntenhöner, M. A. Pogrel, R. Stern, A substrate-gel assay for hyaluronidase activity, Matrix 12 (1992) 388-396.
[88] P. J. Knudsen, P. B. Eriksen, M. Fenger, K. Florentz, High-performance liquid chromatography of hyaluronic acid and oligosaccharides produced by bovine testes hyaluronidase, J. Chromatog. 187 (1980) 373-379.

[89] E. Payan, J. Y. Jouzeau, F. Lapicque, N. Muller, Assay of synovial fluid hyaluronic acid using high-performance liquid chromatography of hyaluronidase digests, J. Chromatog. 566 (1991) 9-18.
[90] A. Suzuki, H. Toyoda, T. Toida, T. Imanari, Preparation and inhibitory activity on hyaluronidase of fully O-sulfated hyaluro-oligosaccharides, Glycobiol. 11 (2001) 57-64.
[91] I. Kakizaki, H. Koizumi, F. Chen, M. Endo, Inhibitory effect of chondroitin sulfate oligosaccharides on bovine testicular hyaluronidase, Carbohydrate Polym. 121 (2015) 362-371.
[92] S. Pattanaargson, J. Roboz, Determination of hyaluronidase activity in venoms using capillary electrophoresis, Toxicon. 34 (1996) 1107-1117.
[93] E. S. A. Hofinger, J. Hoechstetter, M. Oettl, G. Bernhardt, A. Buschauer, Isoenzyme-specific differences in the degradation of hyaluronic acid by mammalian-type hyaluronidases, Glycoconj. J. 25 (2007) 101-109.
[94] M. Koketsu, R. J. Linhardt, Electrophoresis for the analysis of acidic oligosaccharides, Anal. Biochem. 238 (2000) 136-145.
[95] H. Nehmé, S. Chantepie, J. Defert, P. Morin, D. Papy-Garcia, R. Nehmé, New methods based on capillary electrophoresis for in vitro evaluation of protein tau phosphorylation by glycogen synthase kinase 3-β, Anal. Bioanal. Chem. 407 (2014) 2821-2828.
[96] Y. Park, S. Cho, R. J. Linhardt, Exploration of the action pattern of Streptomyces hyaluronate lyase using high-resolution capillary electrophoresis, Biochim. Biophys. Acta 1337 (1997) 217-226.
[97] A. V. Kühn, H. H. Rüttinger, R. H. Neubert, K. Raith, Identification of hyaluronic acid oligosaccharides by direct coupling of capillary electrophoresis with electrospray ion trap mass spectrometry, Rapid Commun. Mass Spectrom. 17 (2003) 576-582.
[98] A. V. Kühn, J.-H. Ozegowski, G. Peschel, R. H. H. Neubert, Complementary exploration of the action pattern of hyaluronate lyase from Streptococcus agalactiae using capillary electrophoresis, gel-permeation chromatography and viscosimetric measurements, Carbohydrate Res. 339 (2004) 2541-2547.
[99] M. Grundmann, M. Rothenhöfer, G. Bernhardt, A. Buschauer, F.-M. Matysik, Fast counter-electroosmotic capillary electrophoresis–time-of-flight mass spectrometry of hyaluronan oligosaccharides, Anal. Bioanal. Chem. 402 (2012) 2617-2623.
[100] J. Matysiak, P. Dereziński, B. Urbaniak, A. Klupczyńska, A. Zalewska, Z. J. Kokot, A new method for determination of hyaluronidase activity in biological samples using capillary zone electrophoresis, Biomed. Chromatogr. 27 (2013) 1070–1078.
[101] S. Pukrittayakamee, D. Warrell, V. Desakorn, A. M. AJ, N. White, D. Bunnag, The hyaluronidase activities of some Southeast Asian snake venoms, Toxicon. 26 (1988) 629-637.
[102] K. P. Vercruysse, A. R. Lauwers, J. M. Demeester, Absolute and empirical determination of the enzymatic activity and kinetic investigation of the action of hyaluronidase on hyaluronan using viscosimetry, Biochem. 306 (1995) 153-160.
[103] S. Fayad, R. Nehmé, M. Langmajerová, B. Ayela, C. Colas, B. Maunit, J.-C. Jacquinet, A. Vibert, C. Lopin-Bon, G. Zdeněk, P. Morin, Hyaluronidase reaction kinetics evaluated by capillary electrophoresis with UV and high-resolution mass spectrometry (HRMS) detection, Anal. Chim. Acta 951 (2017) 140-150.
[104] S. Fayad, R. Nehmé, M. Tannoury, E. Lesellier, C. Pichon, P. Morin, Macroalga Padina pavonica water extracts obtained by pressurized liquid extraction and microwave-assisted extraction inhibit hyaluronidase activity as shown by capillary electrophoresis, J. Chromatogr. A 1497 (2017) 19-27.
[105] Q. Ling, Z. Xue, Z. Jiang-xing, D. Juan, C. Qing-xi, The inhibitory effect on mushroom tyrosinase by the extraction of the inhibitor from the outer Husk of Aloe vera, J. Xiamen Univ. 47 (2008) 227-230.
[106] S. Ito, High-performance liquid chromatography (HPLC) analysis of Eu- and Pheomelanin in melanogenesis control, J. Invest. Dermatol. 100 (1993) 166-171.
[107] A. Salwiński, R. Delépée, B. Maunit, Continuous-flow step gradient mass spectrometry based method for the determination of kinetic parameters of immobilized mushroom tyrosinase in equilibrating conditions: comparison with free enzyme, Rapid Commun. Mass Spectrom. 25 (2011) 3549–3554.
[108] Z. Yang, Y. Zhang, L. Sun, Y. Wang, X. Gao, Y. Cheng, An ultrafiltration high-performance liquid chromatography coupled with diode array detector and mass spectrometry approach for screening and characterising tyrosinase inhibitors from mulberry leaves, Anal. Chim. Acta 719 (2012) 87-95.

[109] Z. Wang, S. H. Hwang, B. Huang, S. S. Lim, Identification of tyrosinase specific inhibitors from Xanthium strumarium fruit extract using ultrafiltration-high performance liquid chromatography, J. Chromatog. B 1002 (2015) 319-328.
[110] A. Salwiński, D. D. Silva, R. Delépée, B. Maunit, The use of enzyme-coupled magnetic nanoparticles for studying the spectra of unusual substrates of mushroom tyrosinase by direct surface-assisted laser desorption/ionisation and high-resolution electrospray ionisation quadrupole-quadrupole-time-of-flight mass spectrometry, Rapid Commun. Mass Spectrom. 28 (2014) 1957-1963.
[111] S. Wangthong, I. Tonsiripakdee, T. Monhaphol, R. Nonthabenjawan, S. P. Wanichwecharungruang, Post TLC developing technique for tyrosinase inhibitor detection, Biomed. Chromatogr. 21 (2007) 94-100.
[112] S. Momtaz, B. M. Mapunya, P. J. Houghton, C. Edgerly, A. Hussein, S. Naidoo, N. Lall, Tyrosinase inhibition by extracts and constituents of Sideroxylon inerme L. stem bark, used in South Africa for skin lightening, J. Ethnopharmacol. 119 (2008) 507-512.
[113] L. Kamagaju, R. Morandini, E. Bizuru, P. Nyetera, J. B. Nduwayezu, C. Stévigny, G. Ghanem, P. Duez, Tyrosinase modulation by five Rwandese herbal medicines traditionally used for skin treatment, J. Ethnopharmacol. 146 (2013) 824-834.
[114] J. Taibon, A. Ankli, S. Schwaiger, C. Magnenat, V.-I. Boka, C. Simões-Pires, N. Aligiannis, M. Cuendet, A.-L. Skaltsounis, E. Reich, H. Stuppner, Prevention of false-positive results: development of an HPTLC autographic assay for the detection of natural tyrosinase inhibitors, Planta Med. 81 (2015) 1198-1204.
[115] E. Chaita, E. Gikas, N. Aligiannis, Integrated HPTLC-based methodology for the tracing of bioactive compounds in herbal extracts employing multivariate chemometrics. A case study on Morus alba, Phytochem. Anal. 28 (2017) 125-131.
[116] V.-I. Boka, K. Stathopoulou, D. Benaki, E. Gikas, N. Aligiannis, E. Mikros, A.-L. Skaltsounis, Could multivariate statistics exploit HPTLC and NMR data to reveal bioactive compounds? The case of *Paeonia mascula*, Phytochem. Lett. (2017).
[117] G. M. Robinson, M. R. Smyth, Simultaneous determination of products and intermediates of L-Dopa oxidation using capillary electrophoresis with diode-array detection, Analyst 122 (1997) 797-802.
[118] W. H. Zhang, Z. H. LV, T. F. Jiang, Y. H. Wang, L. P. Guo, Screening tyrosinase inhibitors from traditional chinese medicine by capillary electrophoresis with electrophoretically mediated microanalysis, J. Food Drug Anal. 20 (2012) 159-163.
[119] B. B. Suna, L. Qi, X. Y. Mu, J. Qiao, M. L. Wang, A chiral ligand exchange CE system for monitoring inhibitory effect of kojic acid on tyrosinase, Talanta 116 (2013) 1121-1125.
[120] Y. Su, X. Mu, L. Qi, A new chiral ligand exchange capillary electrophoresis system based on Zn(II)-L-leucine complexes coordinating with β-cyclodextrin and its application in screening tyrosinase inhibitors, RSC Adv. 4 (2014) 55280-55285.
[121] T.-F. Jiang, T.-T. Liang, Y.-H. Wang, W.-H. Zhang, Z.-H. Lv, Immobilized capillary tyrosinase microreactor for inhibitor screening in natural extracts by capillary electrophoresis, J. Pharm. Biomed. Anal. 84 (2013) 36-40.
[122] M. Cheng, Z. Chen, Screening of tyrosinase inhibitors by capillary electrophoresis with immobilized enzyme microreactor and molecular docking, Electrophoresis 38 (2016) 486-493.

List of figures:

Figure 8: a) Kinetic study of HA degradation by hyaluronidase using CE/UV and CE/HRMS; **b)** Dose-response curves obtained for hyaluronidase inhibition with EGCG using CE/UV and CE/HRMS ($r^2 \geq 0.94$) adapted from [103].
Incubation time: 60 min at 37°C. IB: 2 mM sodium acetate (pH 4.0). BGE: 10 mM ammonium acetate (pH 9.0). Injection at the cathodic side: 0.5 psi for 5 s (18 nL). Electrophoretic separation: - 15 kV at 25°C. Bare-silica capillary: 85 cm x 75 µm i.d.; sheath liquid: MeOH-water (80/20; v/v) with 0.02% formic acid, 10 $\mu L.min^{-1}$; dry gas flow, 6 $L.min^{-1}$; nebulizer pressure: 1.1 bar; ESI voltage: - 4 kV.

Figure 9: Electropherograms obtained for the inhibition of HA hydrolysis by hyaluronidase with different concentrations of pressurized liquid extraction ethyl acetate (a) and water (b) extracts adapted from [104]. Conditions in **Table 2**.

Figure 10: Scheme of ultrafiltration HPLC–DAD–MS assay for screening for tyrosinase inhibitors adapted from [108].

Figure 11: a) TLC results of about 0.5 µg of the 1:1 (w/w) mixture between kojic acid and octyl methoxy-cinnamate adapted from [111]. Mobile phase: 1:1 (v/v) hexane:ethyl acetate. Picture taken under UV light (a) shows kojic acid at the retention value of 0.08 and octyl methoxy-cinnamate at 0.86 and b) after spraying with tyrosinase/L-tyrosine. **b)** 2D-TLC separation of 3 µg of the chloroform Licorice extract. Mobile phase for the first dimension: 60:40 (v/v) methanol:dichlorometahne and 40:60 (v/v) hexane:ethyl acetate as a second dimension mobile phase.

Figure 12: Schematic representation of the immobilized capillary tyrosinase reactor prepared by the LBL assembly adapted from [121].